

# Effect of poling temperature on optical second harmonic intensity of sodium zinc tellurite glasses

Aiko Narazaki, Katsuhisa Tanaka, Kazuyuki Hirao, and Naohiro Soga

*Department of Material Chemistry, Faculty of Engineering, Kyoto University, Sakyo-ku, Kyoto 606-01, Japan*

(Received 7 July 1997; accepted for publication 6 January 1998)

Poling temperature dependence of optical second harmonic intensity has been examined for  $\text{Na}_2\text{O}-\text{ZnO}-\text{TeO}_2$  glasses. All the glasses exhibit such a tendency that the second harmonic intensity increases, experiences a maximum, and decreases as the poling temperature increases. The poling temperature giving rise to the maximum second harmonic intensity, which we call an optimum poling temperature, correlates with glass transition temperature; there exists a linear relation between them. This phenomenon indicates that the structural change of glass network near the glass transition temperature affects the orientation of electric dipoles with a long range order which induces the second harmonic generation. We suggest that some electrochemical reactions take place on the anode-side surface of glass at around the glass transition temperature where viscous flow is allowed and disturb the orientation of electric dipoles. © 1998 American Institute of Physics. [S0021-8979(98)03708-6]

## I. INTRODUCTION

Nonlinear optical properties with second-order of poled glass materials have attracted considerable attention from both fundamental and practical viewpoints since the discovery of second harmonic generation (SHG) in poled silica glass by Myers *et al.*<sup>1</sup> The fundamental interest lies in the fact that an optical anisotropy is induced in glass which has been considered to be a prototype of an optically isotropic solid. From a practical viewpoint, the poled glass will be useful as a frequency doubler of light and a linear electro-optical device. Not only the silica glass<sup>2-6</sup> but also tellurite glass is one of the amorphous materials which exhibit second harmonic generation when the thermal poling is carried out.<sup>7-11</sup> We recently reported poling temperature dependence of optical second harmonic intensity of tellurite glasses in  $\text{MgO}-\text{ZnO}-\text{TeO}_2$  system.<sup>10,11</sup> The second harmonic intensity increases, takes a maximum value, and decreases as the poling temperature increases for all the glass samples studied. A similar phenomenon was observed in poled silica glass.<sup>12</sup> The fact that there exists a poling temperature which gives rise to a maximum second harmonic intensity is important for the production of glass materials with large second-order nonlinear optical susceptibility. However, mechanism for such a variation of optical second harmonic intensity with poling temperature remains obscure. In the case of tellurite glasses, in particular, this phenomenon is interesting in connection with thermally induced change of glass structure because the poling temperature is very close to glass transition temperature.

In the present investigation, we examine the poling temperature dependence of second harmonic intensity for  $30\text{NaO}_{1/2}\cdot 70\text{TeO}_2$  and  $10\text{NaO}_{1/2}\cdot 20\text{ZnO}\cdot 70\text{TeO}_2$  glasses, and discuss the effect of poling temperature on the change of glass structure during the poling. We present our finding that there exists a linear relation between glass transition tem-

perature and the poling temperature corresponding to maximum second harmonic intensity, which is hereafter referred to as an optimum poling temperature.

## II. EXPERIMENTAL PROCEDURE

### A. Sample preparation

Glass samples were prepared from  $\text{Na}_2\text{CO}_3$ ,  $\text{ZnO}$ , and  $\text{TeO}_2$ . The purity of these raw materials was 99.5%, 99%, and 99%. The raw materials were mixed thoroughly to make  $30\text{NaO}_{1/2}\cdot 70\text{TeO}_2$  and  $10\text{NaO}_{1/2}\cdot 20\text{ZnO}\cdot 70\text{TeO}_2$  compositions, and melted in a platinum crucible at 850 °C for 20 min in air. The melt was poured onto a carbon plate to obtain glass. The glass transition temperature was measured using differential thermal analysis (Rigaku, TG-DTA8112BH). After the glass was annealed at around the glass transition temperature for 20 min, it was cut into a plate. Both surfaces of the platelike glass were polished to make a specimen for measurements of second harmonic generation. The thickness of the resultant glass sample was 1 mm.

Poling of the glass sample was performed as follows. The glass sample was sandwiched in between two commercial borosilicate glass plates and contacted physically with electrodes made of stainless steel. The commercial borosilicate glass plates were used to avoid precipitation of metallic tellurium which occurred on the cathode-side glass surface when the glass sample was contacted directly to the electrodes made of stainless steel.<sup>9</sup> The use of commercial borosilicate glass plates was also effective to avoid discharge between the electrodes. The glass sample sandwiched with the electrodes was put into an electric furnace and heated to an aimed temperature. After the glass sample was held at the temperature for 30 min, the voltage of 3 kV was applied for 20 min. Then, the glass sample was taken out from the furnace and quenched to room temperature while the constant voltage was applied. The voltage was removed after the tem-

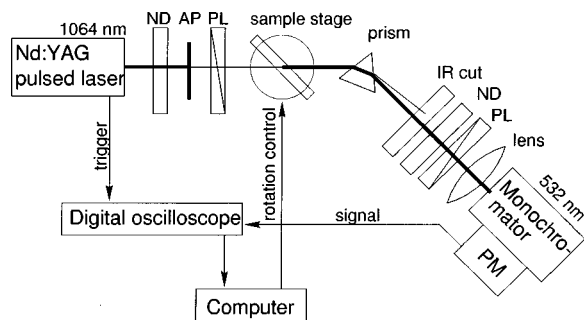


FIG. 1. Schematic illustration of equipment for second harmonic generation measurements. The output beam is split into second harmonic wave (thick line) and fundamental wave (thin line) by the prism. The meanings of abbreviations are as follows. ND: ND filter; AP: aperture; PL: polarizer; IR cut: IR cut filter; and PM: photomultiplier.

perature of the glass sample was decreased to the room temperature. It should be noted that the actual voltage applied to the glass sample was less than 3 kV because the glass sample was sandwiched with two commercial glass plates as mentioned above.

## B. Measurements

The second harmonic intensity of poled glass samples was measured using Maker fringe method.<sup>13</sup> A setup for SHG measurements is illustrated schematically in Fig. 1. The intensity of second harmonic wave from poled glass sample was measured using a pulsed Nd:YAG laser (Spectra Physics, GCR-11) which operated in a Q-switched mode with a 10 Hz repetition rate. The incident pulse was a *p*-excited fundamental wave at 1064 nm with 9 ns duration. The output light from the poled glass was passed through a prism to divide the second harmonic wave with 532 nm from the fundamental wave. The *p*-polarized second harmonic wave was passed through a monochromator (Spex, 270M) and detected with a photomultiplier (Hamamatu Photonics, R955). The signal from the photomultiplier was accumulated by using a digital oscilloscope (Hewlett Packard 54522A). In order to perform the Maker fringe measurement the poled sample was rotated on *x* axis, which is arranged parallel to the sample surface, from  $-65^\circ$  to  $65^\circ$ . For the determination

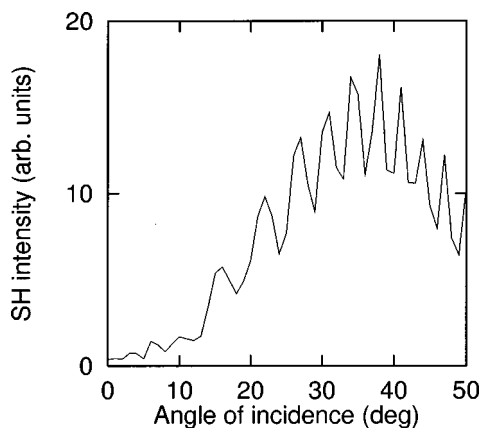


FIG. 2. Maker fringe pattern of  $30\text{NaO}_{1/2}\cdot 70\text{TeO}_2$  glass poled at  $220^\circ\text{C}$  with 3 kV.

TABLE I. Glass composition, glass transition temperature, and optimum poling temperature of  $\text{Na}_2\text{O}-\text{ZnO}-\text{TeO}_2$  glasses.

Glass composition (mol %)	Glass transition temperature ( $^\circ\text{C}$ )	Optimum poling temperature ( $^\circ\text{C}$ )
$30\text{NaO}_{1/2}\cdot 70\text{TeO}_2$	250	225
$10\text{NaO}_{1/2}\cdot 20\text{ZnO}\cdot 70\text{TeO}_2$	300	260
$30\text{ZnO}\cdot 70\text{TeO}_2^a$	326	280

<sup>a</sup>Cited in Ref. 10.

of input light power, Y-cut quartz with thickness of 1.046 mm and  $d_{11}=0.34$  pm/V was used as a reference material under the condition of *p*-excitation and *p*-detection.

X-ray diffraction measurements were carried out for both as-annealed and poled glasses with Cu  $K\alpha$  radiation (Rigaku, RAD-C). For each surface of bulk sample, diffraction angle was scanned from  $2\theta=10$  to  $70^\circ$  at intervals of  $0.05^\circ$ . The scan speed was  $2^\circ/\text{min}$ .

Refractive indices at 532 and 1064 nm were measured by using an ellipsometer (Yokojiri, DVA-36VW) for poled glass samples to estimate second-order nonlinear optical coefficient.

## III. RESULTS

Table I shows glass transition temperature of  $\text{Na}_2\text{O}-\text{ZnO}-\text{TeO}_2$  glasses. The glass transition temperature increases with a replacement of Na by Zn. The variation of second harmonic intensity with angle of incidence for  $30\text{NaO}_{1/2}\cdot 70\text{TeO}_2$  glass poled at  $220^\circ\text{C}$  with 3 kV is shown in Fig. 2. The Maker fringe pattern is observed, although minimum values of intensity are not zero in contrast with the theory of Maker fringe. For  $30\text{NaO}_{1/2}\cdot 70\text{TeO}_2$  glass poled at  $225^\circ\text{C}$ , the dependence of second harmonic intensity on incident angle is shown in Fig. 3. When the anode-side surface of this glass was etched mechanically with about  $30\ \mu\text{m}$ , the second harmonic generation disappeared, which indicates that the origin of SHG exists in thin layer near the anode-side surface. In this figure, the solid curve is a theoretical one drawn by using the refractive indices shown in Table II and

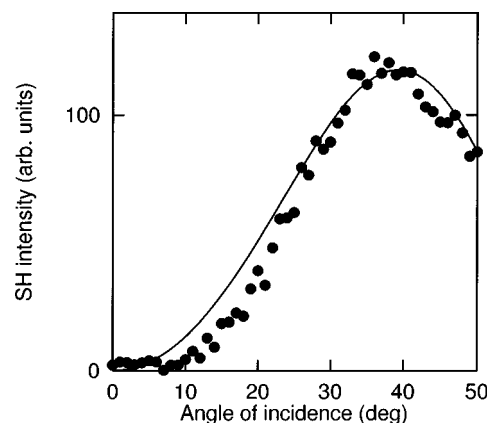


FIG. 3. Maker fringe pattern of  $30\text{NaO}_{1/2}\cdot 70\text{TeO}_2$  glass poled at  $225^\circ\text{C}$  with 3 kV. The circles denote the fringe pattern obtained experimentally. The solid curve represents the theoretical fringe pattern drawn with  $d_{33}=0.082$  pm/V,  $L=28\ \mu\text{m}$ ,  $n_{532}=2.00$  and  $n_{1064}=1.95$ .

TABLE II. Refractive indices at 532 and 1064 nm ( $n_{532}$  and  $n_{1064}$ ) and  $d_{33}$  values of poled  $\text{Na}_2\text{O}-\text{ZnO}-\text{TeO}_2$  glasses. Each glass was poled at the optimum poling temperature listed in Table I.

Glass composition	$n_{532}$	$n_{1064}$	$d_{33}$ (pm/V)
$30\text{NaO}_{1/2}\cdot 70\text{TeO}_2$	2.00	1.95	0.082
$10\text{NaO}_{1/2}\cdot 20\text{ZnO}\cdot 70\text{TeO}_2$	2.02	1.97	0.23
$30\text{ZnO}\cdot 70\text{TeO}_2$	2.05	2.00	0.45

by assuming that the poled region is  $28\ \mu\text{m}$ . This value,  $28\ \mu\text{m}$ , is coincident with the fact that the mechanical etching of  $30\ \mu\text{m}$  of anode-side glass surface makes the second harmonic wave disappear. The agreement between the experimental data and theoretical curve is rather good. From this analysis,  $d_{33}=0.082\ \text{pm/V}$  is obtained. Figure 4 shows the dependence of second harmonic intensity on angle of incidence for  $30\text{ZnO}\cdot 70\text{TeO}_2$  glass poled at  $280^\circ\text{C}$ . The solid circles denote experimental result, and the solid curve represents theoretical one drawn with  $L=27\ \mu\text{m}$  and  $d_{33}=0.45\ \text{pm/V}$ , where  $L$  is the length of poled region. The values of  $d_{33}$  thus obtained are summarized in Table II.

The variation of second harmonic intensity with poling temperature for  $30\text{NaO}_{1/2}\cdot 70\text{TeO}_2$  glass is shown in Fig. 5. The second harmonic intensity exhibits a maximum at  $225^\circ\text{C}$  which is  $25^\circ\text{C}$  below the glass transition temperature. In other words, the optimum poling temperature is  $225^\circ\text{C}$ . Figure 6 shows the variation of second harmonic intensity with poling temperature for  $10\text{NaO}_{1/2}\cdot 20\text{ZnO}\cdot 70\text{TeO}_2$  glass. This glass manifests a maximum of second harmonic intensity as well and the optimum poling temperature is  $260^\circ\text{C}$ . The optimum poling temperature of  $\text{Na}_2\text{O}-\text{ZnO}-\text{TeO}_2$  glasses is summarized in Table I.

In poled  $30\text{NaO}_{1/2}\cdot 70\text{TeO}_2$  glasses, devitrification was observed at the anode-side glass surface. Figure 7 shows x-ray diffraction patterns of as-annealed glass sample and the anode-side surface of poled glass samples with  $30\text{NaO}_{1/2}\cdot 70\text{TeO}_2$  composition. Two peaks at around  $2\theta=18.4^\circ$  and  $27.7^\circ$  can be assigned to  $\text{Te}_4\text{O}_9$  and  $\text{TeO}_2$  crys-

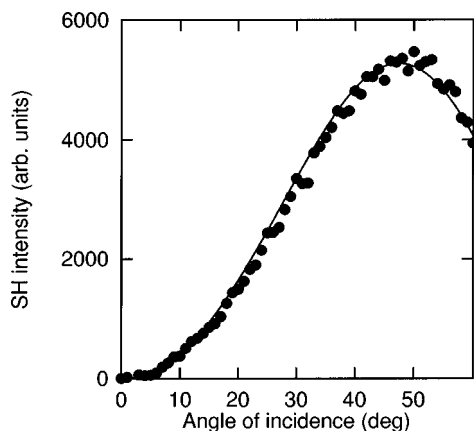


FIG. 4. Maker fringe pattern of  $30\text{ZnO}\cdot 70\text{TeO}_2$  glass poled at  $280^\circ\text{C}$  with 3 kV. The circles and solid curve denote the experimental and theoretical Maker fringe patterns, respectively. The theoretical one was drawn with  $d_{33}=0.45\ \text{pm/V}$ ,  $L=27\ \mu\text{m}$ ,  $n_{532}=2.05$  and  $n_{1064}=2.00$ .

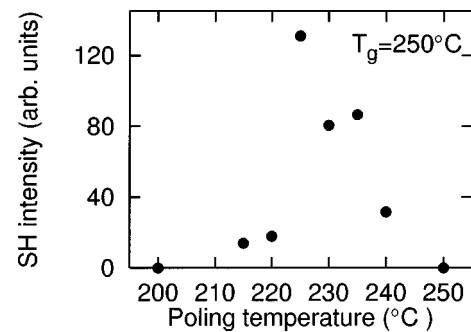


FIG. 5. Poling temperature dependence of second harmonic intensity for  $30\text{NaO}_{1/2}\cdot 70\text{TeO}_2$  glass poled with 3 kV for 20 min.

tal, respectively. This fact clearly indicates that some electrochemical reactions occurred at interface between anode and glass surface and these reactions become vigorous when the poling temperature is increased.

#### IV. DISCUSSION

As for the poled silica glasses, the initial stage of poling is migration of cations such as  $\text{Na}^+$ , as suggested by Myers *et al.*<sup>1</sup> The migration of cations leaves thin space charge layer near the anode, and the external voltage drops drastically in this region. In other words, a large electric field is applied to the thin layer in the glass near the anode. This large electric field is frozen in the anode-side surface region of the glass, leading to the second harmonic generation.<sup>1</sup> This phenomenon can take place in the tellurite glasses containing mobile cations such as  $\text{Na}^+$  and  $\text{Zn}^{2+}$  as well. The electric dipoles created as a result of pairing of these mobile cations with nonbridging oxide ions can contribute to the second harmonic generation. In addition, the large electric field in the anode-side glass surface region possibly leads to an orientation of asymmetrical tellurite structural units such as  $\text{TeO}_4$  trigonal bipyramid and  $\text{TeO}_3$  trigonal pyramid which possess electric dipoles because the poling is performed near the glass transition temperature. In particular, these structural units with nonbridging oxygens can be readily oriented by the electric field. We suggest that these electric dipoles bring about the second harmonic generation as shown in Figs. 2, 3, and 4.

Like  $\text{MgO}-\text{ZnO}-\text{TeO}_2$  glass system reported previously,<sup>10,11</sup> the  $\text{Na}_2\text{O}-\text{ZnO}-\text{TeO}_2$  glasses show a pecu-

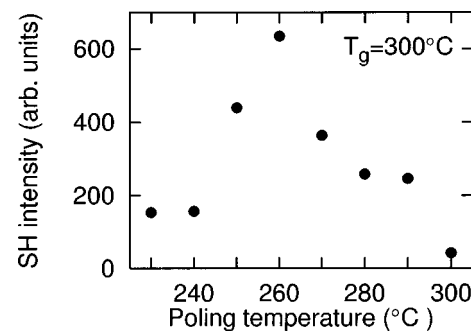


FIG. 6. Poling temperature dependence of second harmonic intensity for  $10\text{NaO}_{1/2}\cdot 20\text{ZnO}\cdot 70\text{TeO}_2$  glass poled with 3 kV for 20 min.

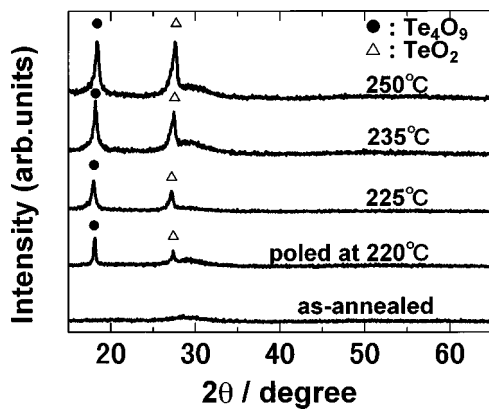


FIG. 7. X-ray diffraction patterns of as-annealed and poled  $30\text{NaO}_{1/2}\cdot 70\text{TeO}_2$  glasses. The surfaces of bulk glasses were examined in these measurements. It should be noted that for poled glasses devitrification is observed only at the anode-side surface. The circle and triangle denote the diffraction lines of  $\text{Te}_4\text{O}_9$  and  $\text{TeO}_2$  crystals, respectively.

liar dependence of second harmonic intensity on poling temperature; both systems possess optimum poling temperature. Namely, the second harmonic intensity increases as the poling temperature increases up to the optimum poling temperature and becomes almost zero when the poling temperature is close to the glass transition temperature. The increase in second harmonic intensity with an increase in poling temperature below the optimum poling temperature can be naturally attributed to an increase in mobility of cations, which form large electric dipoles.

Figure 8 shows the relationship between optimum poling temperature and glass transition temperature for the  $\text{MgO-ZnO-TeO}_2$  glasses as well as the present  $\text{Na}_2\text{O-ZnO-TeO}_2$  glasses. The optimum poling temperature is proportional to the glass transition temperature. This experimental fact clearly indicates that the formation and orientation of electric dipoles is closely related to the structural relaxation at around the glass transition temperature. One possible mechanism to explain the poling temperature dependence of second harmonic intensity and the relationship between optimum poling temperature and glass transition temperature is the effect of thermal fluctuation on the orientation

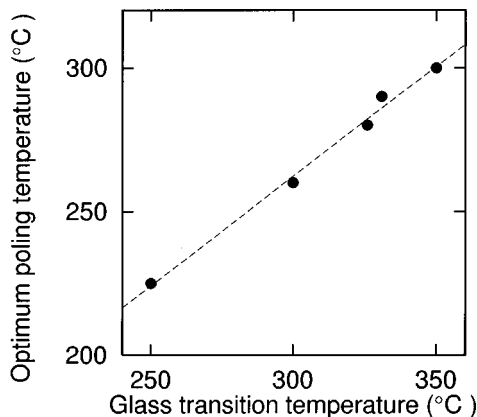


FIG. 8. Relation between optimum poling temperature and glass transition temperature observed in  $\text{Na}_2\text{O-ZnO-TeO}_2$  and  $\text{MgO-ZnO-TeO}_2$  glass systems. The broken line was drawn by the method of least squares.

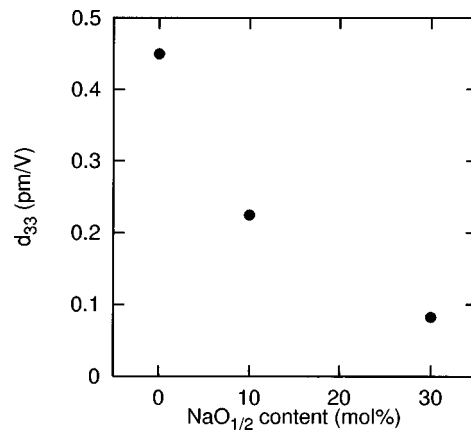


FIG. 9. Compositional dependence of second-order nonlinear optical coefficient for  $x\text{NaO}_{1/2}\cdot (30-x)\text{ZnO}\cdot 70\text{TeO}_2$  glasses ( $x=0,10,30$ ) poled at the optimum poling temperature with 3 kV.

of electric dipoles at higher temperatures as argued previously.<sup>10,11</sup> Another possible explanation, which we believe more plausible, includes electrochemical reactions between glass surfaces and electrodes at higher temperatures. As shown in Fig. 7, the precipitation of  $\text{Te}_4\text{O}_9$  and  $\text{TeO}_2$  crystals was observed at the anode-side surface of poled  $30\text{NaO}_{1/2}\cdot 70\text{TeO}_2$  glasses. This indicates that an irreversible electrochemical reaction occurs at the interface between anode and glass surface. In particular, the precipitation of  $\text{Te}_4\text{O}_9$  suggests that some oxidation reaction takes place. Further, the amount of precipitation became larger as the poling temperature increased. The oxidation reactions at around the anode-side surface of glass reduce the effect of external electric field, and subsequently, hinder the formation and orientation of electric dipoles. In addition, the reactions occur more efficiently as the temperature becomes higher. Consequently, the second harmonic intensity decreases as the temperature increases above the optimum poling temperature. In particular, the electrochemical reactions to reduce the second harmonic intensity become rather active in the vicinity of the glass transition temperature at which viscous flow begins to occur. Hence, the optimum poling temperature increases monotonically with an increase in the glass transition temperature.

For  $\text{Na}_2\text{O-ZnO-TeO}_2$  glasses, the maximum second-order nonlinear optical coefficients are compared with each other in Fig. 9. The second-order nonlinear optical coefficient increases with a replacement of  $\text{NaO}_{1/2}$  by  $\text{ZnO}$ . This increase can be attributed to the rise in the content of nonbridging oxygens,<sup>14</sup> which contribute to the dipole moments oriented under the dc electric field, and lead to the anisotropic structure. In this viewpoint, a glass containing a large number of nonbridging oxygens has a good ability to generate large anisotropy. In addition, high mobility of  $\text{Na}^+$  enhances the electrochemical reactions at high temperatures, leading to a decrease in the second harmonic intensity as well as the second-order nonlinear optical coefficient observed for the glasses with a large amount of  $\text{Na}_2\text{O}$ .

## V. CONCLUSIONS

The second harmonic intensity was measured using the Maker fringe method for Na<sub>2</sub>O–ZnO–TeO<sub>2</sub> glasses poled at several temperatures. The dependence of second harmonic intensity on the poling temperature observed in the Na<sub>2</sub>O–ZnO–TeO<sub>2</sub> glasses is similar to that of MgO–ZnO–TeO<sub>2</sub> glasses reported previously. When the poling temperature is low, the second harmonic intensity increases with an increase in the poling temperature, and exhibits a maximum at the optimum poling temperature. Then, the intensity becomes almost zero when the poling temperature reaches the glass transition temperature. This decrease in second harmonic intensity suggests that some electrochemical reactions at the anode-side surface break up the region where electric dipoles are oriented when the poling temperature approaches the glass transition temperature. We found that the optimum poling temperature is proportional to the glass transition temperature.

## ACKNOWLEDGMENTS

The authors would like to thank Professor T. Yoko of Institute for Chemical Research, Kyoto University, for the measurements of refractive index. They are also indebted to

Professor T. Kokubo of Faculty of Engineering, Kyoto University, for the x-ray diffraction measurements.

- <sup>1</sup>R. A. Myers, N. Mukherjee, and S. R. J. Brueck, *Opt. Lett.* **16**, 1732 (1991).
- <sup>2</sup>H. Nasu, H. Okamoto, A. Mito, J. Matsuoka, and K. Kamiya, *Jpn. J. Appl. Phys., Part 2* **32**, L406 (1993).
- <sup>3</sup>A. Okada, K. Ishii, K. Mito, and K. Sasaki, *Appl. Phys. Lett.* **60**, 2853 (1992).
- <sup>4</sup>P. G. Kazansky, L. Dong, and P. St. J. Russell, *Electron. Lett.* **30**, 1345 (1994).
- <sup>5</sup>O. Sugihara, T. Hirama, H. Fujimura, and N. Okamoto, *Opt. Rev.* **3**, 150 (1996).
- <sup>6</sup>H. Takebe, P. G. Kazansky, and P. S. J. Russell, *Opt. Lett.* **21**, 468 (1996).
- <sup>7</sup>K. Tanaka, K. Kashima, K. Hirao, N. Soga, A. Mito, and H. Nasu, *Jpn. J. Appl. Phys., Part 2* **32**, L843 (1993).
- <sup>8</sup>K. Tanaka, K. Kashima, K. Kajihara, K. Hirao, N. Soga, A. Mito, and H. Nasu, *Proc. SPIE* **2289**, 167 (1994).
- <sup>9</sup>K. Tanaka, K. Kashima, K. Hirao, N. Soga, A. Mito, and H. Nasu, *J. Non-Cryst. Solids* **185**, 123 (1995).
- <sup>10</sup>K. Tanaka, A. Narazaki, K. Hirao, and N. Soga, *J. Appl. Phys.* **79**, 3798 (1996).
- <sup>11</sup>K. Tanaka, A. Narazaki, K. Hirao, and N. Soga, *J. Non-Cryst. Solids* **203**, 49 (1996).
- <sup>12</sup>R. A. Myers, X. Long, and S. R. J. Brueck, *Proc. SPIE* **2289**, 98 (1994).
- <sup>13</sup>P. D. Maker, R. W. Terhune, M. Nisenoff, and C. M. Savage, *Phys. Rev. Lett.* **8**, 21 (1962).
- <sup>14</sup>A. Osaka, J. Qiu, T. Fujii, T. Nanba, J. Takada, and Y. Miura, *J. Soc. Mater. Sci. Jpn.* **42**, 473 (1993).